



Contents lists available at ScienceDirect

## Renewable and Sustainable Energy Reviews

journal homepage: [www.elsevier.com/locate/rser](http://www.elsevier.com/locate/rser)

## A review of nonimaging solar concentrators for stationary and passive tracking applications

Srikanth Madala\*, Robert F. Boehm

Center for Energy Research, Department of Mechanical Engineering, University of Nevada, Las Vegas 89154-4027, United States

## ARTICLE INFO

## Keywords:

Solar concentrators  
 Nonimaging optics  
 CPC  
 Compound parabolic concentrator  
 V-trough  
 Polygonal trough  
 Concentration ratio  
 Non-tracking solar concentrators  
 Stationary solar concentrators  
 CHC  
 CEC  
 Compound hyperbolic concentrators  
 Compound elliptical concentrators  
 Nonimaging Fresnel lenses  
 Dielectric compound parabolic concentrators  
 DCPC  
 Trumpet-shaped concentrators

## ABSTRACT

The solar energy research community has realized the redundancy of image-forming while collecting/concentrating solar energy with the discovery of the nonimaging type radiation collection mechanism in 1965. Since then, various nonimaging concentration mechanisms have proven their superior collection efficiency over their imaging counter-parts. The feasibility of using nonimaging concentrators successfully for stationary applications has rekindled interest in them. The economic benefits are appealing owing to the elimination of tracking costs (installation, operation & maintenance and auxiliary energy). This paper is an exhaustive review of the available nonimaging concentrating mechanisms with stationary applications in mind. This paper also explores the idea of coupling nonimaging concentrators with passive solar tracking mechanism.

### 1. Introduction

Amongst the total solar electric power worldwide today (as per 2015 data) [1], solar photovoltaics (PV) contribute about 227 GW, and concentrating solar power (CSP) technologies contribute about 4.8 GW in generation capacity. NREL's SolarPACES program constantly monitors and updates the global list of CSP projects that are either operational or currently under development [2]. The parabolic trough (an imaging-type solar concentrator technology) accounts for a vast majority of the CSP installations worldwide due to its cost advantage, although power tower systems are quickly catching up. United States and Spain being the front-runners, various other nations including the Middle East and North Africa (MENA) countries, South Africa, India, and China are fast adopting CSP [3].

No matter the type of CSP technology adopted, actively tracking the Sun in order to achieve meaningful concentration is a common trait in all of them. The concentration of solar radiation is typically achieved by using an active solar tracking mechanism coupled with a point- or line-focus imaging concentration system. However, even the best of the

traditional imaging techniques of concentration fall short of the thermodynamic limit of maximum attainable concentration at least by a factor of four due to severe off-axis aberration and coma causing image blurring and broadening. Imaging is an inhibitive phenomenon as far as only energy concentration is concerned. The concentration of solar energy does not demand imaging qualities, but instead requires flexible concentrator designs coping with solar disk size, solar spectrum, and tracking errors while delivering a highly uniform flux [4]. Moreover, an active solar tracking mechanism, often accompanying an imaging concentrator, also adds to the capital and O&M costs while consuming a fraction of the power produced. Therefore, with all these disadvantages in view, nonimaging and stationary techniques of concentrating solar radiation are sought after.

Nonimaging concentrators have been used in solar energy collection systems ever since their discovery in 1965. In the decades that followed, various nonimaging concentrator designs were discovered and evaluated as stationary installations. The concentration ratios achieved were typical low (< 3X) or medium (3-10X). However, the application of these types of concentrators on a large scale or a utility

\* Corresponding author.

E-mail address: [srikant.madala@gmail.com](mailto:srikant.madala@gmail.com) (S. Madala).<http://dx.doi.org/10.1016/j.rser.2016.12.058>Received 6 February 2016; Received in revised form 14 November 2016; Accepted 8 December 2016  
1364-0321/© 2016 Elsevier Ltd. All rights reserved.

**Nomenclature**

CPC	Compound Parabolic Concentrator
ACPC	Asymmetric Compound Parabolic Concentrator
BIPV	Building Integrated Photovoltaics
CCAC	Compound Circular Arc Concentrator
CEC	Compound Elliptical Concentrator
CHC	Compound Hyperbolic Concentrator
CPV	Concentrated Photovoltaics
CR	Concentration Ratio
CSP	Concentrated Solar Power
CSP	Concentrated Solar Power
$d_1$	Dimension of Entrance Aperture
$d_2$	Dimension of Exit Aperture
DACPC	Dielectric Asymmetric Parabolic Concentrator
DCPC	Dielectric Compound Parabolic Concentrator
ER	Energy Ratio
$F(\theta)$	Angular Acceptance Function
FDTD	Finite-Difference Time-Domain
GW	Giga Watt
H	Height of the CPC
$h_c$	Convective Heat Transfer Coefficient

$h_{cd}$	Conductive Heat Transfer Coefficient
$h_R$	Radiative Heat Transfer Coefficient
$h_{tot}$	Overall Heat Transfer Coefficient
$H_{trunc}$	Height of the truncated CPC
LVT	Lens-V Trough
MENA	Middle East and North Africa
$n$	Refractive Index of the Dielectric Media
NREL	National Renewable Energy Laboratory
O&M	Operation and Maintenance
PCCPC	Prism-coupled Compound Parabolic Concentrator
PV	Photovoltaics
R	Reflector-To-Aperture Ratio
SPC	Simple Parabolic Concentrator
$\alpha$	Absorptivity
$\beta$	Prism Apex Angle
$\delta$	Complete Acceptance Angle of V-trough
$\varepsilon$	Emissivity
$\theta$	Angle of Incidence of an Arbitrary Light Ray
$\theta_{aor} \theta_{max}$	Acceptance Angle
$\theta_d$	Truncated CPC's Edge Ray Angle
$\Phi$	Half Angle Of The V-Shaped Cone

scale is yet to be materialized. This current paper is a review of the presently existing and upcoming nonimaging techniques for concentration of solar radiation in stationary or passive tracking applications. Novel applications, and modern techniques of raytracing analysis on nonimaging concentrators has also been discussed as a part of this review.

## 2. Stationary solar energy collectors

Stationary solar energy collector designs such as a flat plate and a concentric cylindrical tube have been prevalent in low temperature ( $< 200^\circ\text{F}$ ) applications such as solar domestic/pool water heating, dehydration of agricultural products, etc. since the beginning of the 20<sup>th</sup> century [5]. As early as the mid-1970s, Falbel Energy System Corp. manufactured a stationary 'nonimaging' collector (called the FES delta solar collector) with a cylindrical cavity trough that achieved a net gain of 2.3X compared to a flat plate collector. Another company named Kaptron manufactured a modified stationary flat-plate solar collector by incorporating a window with optical ribs, an optical valve and a multi-reflection absorber enclosed in an insulated casing, thus making it more efficient over a conventional design [6]. In more recent times, a Stationary V-trough collector (cone angle= $60^\circ$ ) was fabricated and tested in a solar water heating application for the geographical location of Kuala Lumpur ( $3.2^\circ\text{N}$  and  $101^\circ 44' \text{E}$ ) [7]. The collector was oriented in the E-W direction with  $0^\circ$  tilt angle. With a surface area of  $0.56 \text{ m}^2$ , it achieved a diurnal power collection that varied between 0.154 and 0.261 kW. When compared with respect to a flat-plate absorber, the average relative solar concentration ratios of the V-trough varied between 1.19 and 1.85 throughout the year. Interestingly, the peak summer and winter months saw a decrement in the relative concentration ratio.

## 3. Nonimaging solar concentrators

Nonimaging concentrators are a classification of radiation collectors that direct the radiative energy passing the entry aperture (larger area,  $A_1$ ) of the concentration system through to the exit aperture (smaller area,  $A_2$ ) with minimum optical losses. The term 'nonimaging' or 'anidolic' (from Greek an: without, eidolon: image) refers to the virtue of the concentration system to focus the étendue or 'throughput' on a wider area rather than a single focal point and, thus, unable to

form an image of the light source. Unlike the conventional imaging concentration systems, the quality of the image at the exit aperture is of least importance in these concentrators. An illustration of a hypothetical nonimaging concentration system is shown in Fig. 1. The concept of nonimaging collection of radiation came into the picture when the compound parabolic concentrator (CPC) was proposed by Hinterberg and Winston in 1965 as an efficient means of measuring Čerenkov radiation. The early 70s saw a tremendous rise in the number of researchers experimenting on application of various CPC/modified CPC designs as solar concentrators. All these nonimaging collector designs obey a fundamental principle known as the edge-ray principle (used in the design of nonimaging optics) which can be summed up as: "if the edge or boundary rays from a source to an optical system (reflective or refractive) are able to be directed to the edges of a target area, then all the rays in between these edge rays will also be directed to the target area". Winston et al. [8] demonstrated the edge-ray principle using the string method. The same principle has also been refined by using a topological approach [9].

The properties of various nonimaging CPC-type concentrators including the compound elliptical concentrator (CEC), compound hyperbolic concentrator (CHC), trumpet-shaped concentrator and generalized involute reflectors were discussed by Gordon and Rabl [10]. A comparative review on various reflective type solar concentrators has been reported as well [11]. Collector characteristics such as geometric concentration ratio, acceptance angle, sensitivity to mirror

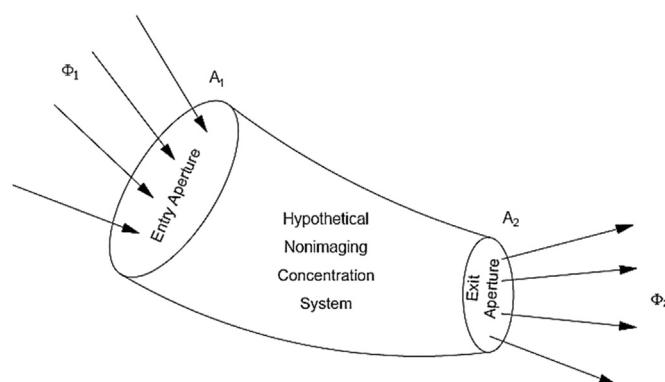


Fig. 1. Illustration of a nonimaging concentration system with entry flux ( $\Phi_1$ ) and exit flux ( $\Phi_2$ ).

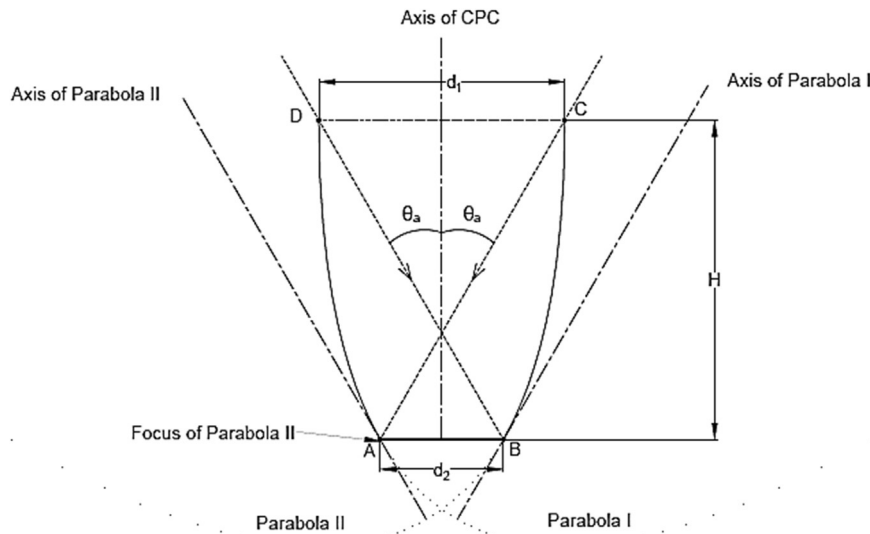


Fig. 2. A compound parabolic concentrator.

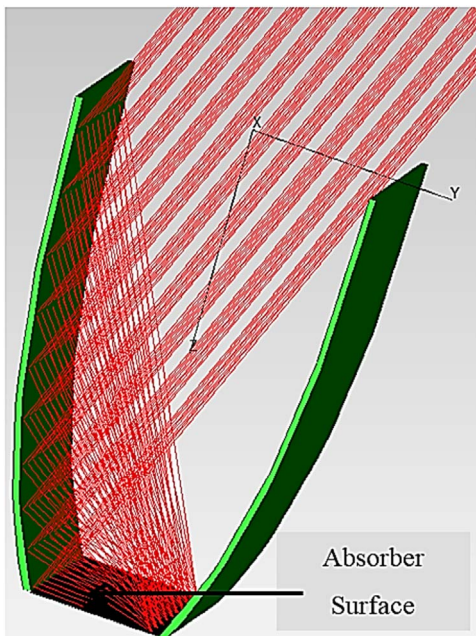


Fig. 3. TracePro illustration of the working principle of hollow CPC concentrator.

errors, reflector area, and average number of reflections were compared. The family of compound parabolic concentrators (CPCs) with various reflector and absorber geometries, Fresnel mirrors, V-trough concentrators and conventional imaging type concentrator designs such as parabolic trough were discussed in this review. Furthermore, two-stage concentration systems with Fresnel mirrors as a primary stage and CPC or V-trough as a secondary stage were also discussed. More recently, O’Gallagher [12] described various nonimaging collector designs in his retrospection of the research work carried out at the University of Chicago during the past 30 years. A review on solar photovoltaic concentrators briefly discussed a few designs of nonimaging concentrators such as CPC, CHC, quantum dot concentrator, dielectric total internally reflecting concentrator (DTIRC), and multi-stage concentrators [13]. Another similar review also presented a few more nonimaging concentrator designs for concentrated photovoltaic application [14]. The convex-shaped nonimaging Fresnel lens, and various other innovative multistage collector designs were discussed. The following sub-sections describe a few prominent existing and

upcoming designs of nonimaging concentrators in greater detail with stationary or passive tracking application in perspective.

### 3.1. Compound parabolic concentrator

The basic design of a CPC concentrator is as shown in Fig. 2. AD and BC are two different parabolic profiles with foci at the end points of the exit aperture – B and A respectively. The tangential lines with respect to BC and AD at the end points of exit aperture – B and A – form the axes of the parabolas AD and BC respectively. A ray-tracing analysis of a hollow CPC (often referred to as a 2D CPC as it focuses on to a 2D plane) is shown in Fig. 3. The CPC attracted immediate attention of the solar energy research community with a capability of concentrating solar radiation by a factor of  $\sim 10$  with just seasonal adjustment and minimal diurnal tracking [15]. For a stationary CPC, a concentration factor of  $\sim 3$  is quite plausible. Also, the efficiency of accepting diffuse solar radiation enhanced further interest in their study.

#### 3.1.1. Comparison of CPCs with other solar collectors

The comparison between a simple parabolic concentrator (SPC) and a compound parabolic concentrator (CPC) has been made to show how the geometric concentration ratio of the SPC is lower by at least a factor of  $\pi$  compared to the CPC with same acceptance angle [16]. A simple calculation shows that for a case of concentration ratio,  $CR=10$ , a CPC uses 4.4 times the amount of material used by a SPC. However, CPC also has 3.15 times more acceptance angle for the same case.

A typical limiting value of concentration ratios of CPCs and SPCs in order to enable collection of circumsolar radiation was calculated to be 19.1 and 6.1 respectively which corresponds to an acceptance angle of  $3^\circ$  [16]. The reason for this limit being that the typical additional amount of circumsolar radiation available at smaller acceptance angles of  $1^\circ$ ,  $2^\circ$  and  $3^\circ$  are 13%, 20% and 22% more than that compared to the intensity of the solar disk alone (solar disk  $\sim 4.65 \times 10^{-3}$  rad or  $0.266^\circ$ ). Beyond a  $3^\circ$  acceptance angle, the effect of circumsolar radiation is negligible.

A large-area ( $13.6 \text{ m}^2$ ) of stationary CPC collector (with flat absorbers) was compared against a stationary flat plate collector, both collectors oriented in E-W direction [17]. The CPC recorded a thermal loss coefficient that is  $0.8 \text{ W/m}^2/\text{K}$  lower than the flat-plate collector owing to the absorption of solar radiation by the reflectors and thus smaller losses to the cover from the absorber surface. Usage of low emissive reflectors and Teflon film as a transparent insulation between the cover and the absorber were the measures to improve the

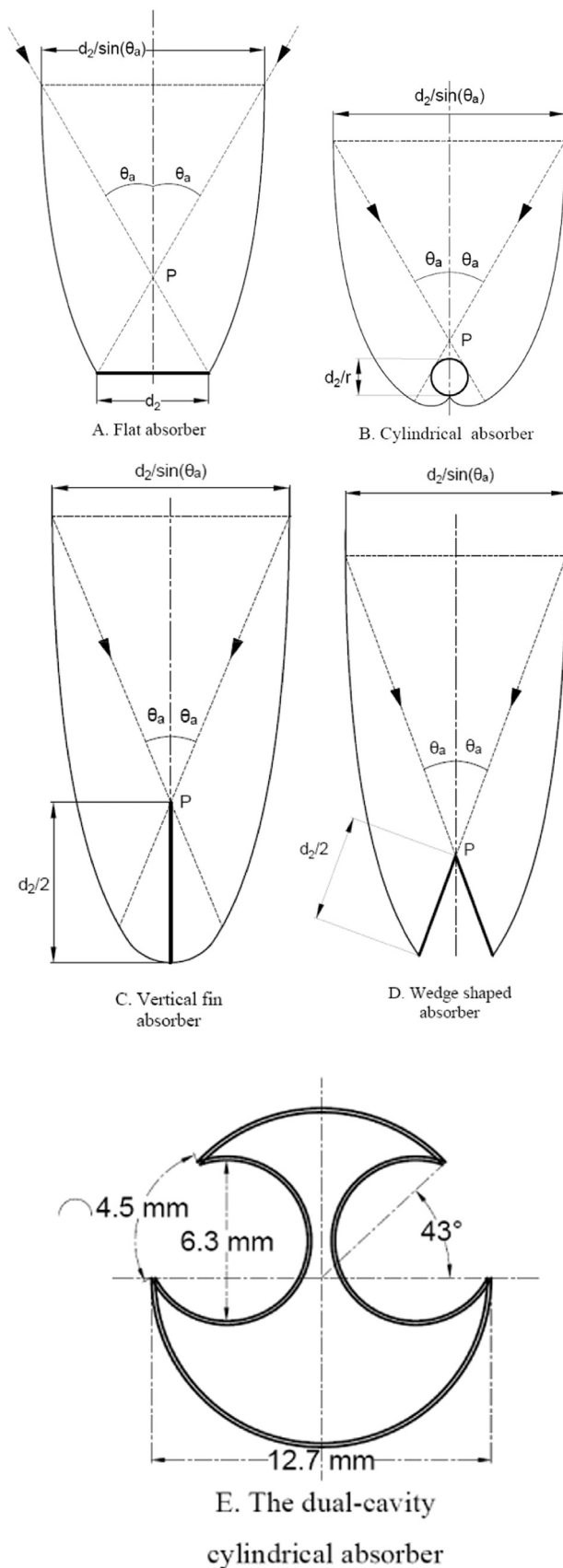


Fig. 4. Various absorber geometries used in CPCs [18,19].

performance. The optical efficiency of the considered CPC ( $\theta_a=35^\circ$ ,  $CR=1.53$ ) was about 0.75 compared to 0.80 of its flat-plate counterpart. The difference in optical performance was too minor to compare given the fact that different types of material were used in the two collectors.

### 3.1.2. Experimentation with CPC absorber designs

Various types of absorbers (viz. flat plate, cylindrical etc.) are used depending on the application of the CPC collector. Some of the commonly used absorber cross-sectional geometries are shown in Fig. 4, where Fig. 4A, Fig. 4B, Fig. 4C and Fig. 4D show flat, cylindrical, vertical fin, and wedge-shaped absorber geometries that are more common while Fig. 4E shows a non-typical dual-cavity absorber that is used with a CPC [18].

The dual-cavity absorber (enlarged geometry as shown in Fig. 4E) was tested against a cylindrical absorber of similar dimensions on a CPC under same test conditions [19]. An improvement in the optical efficiency by about 15–17% is reported for paraxial irradiance. This type of absorber design may be useful when coupled with an active tracking CPC.

Some other commonly used absorber designs such as the bottom tube sheet and the top embossed honeycomb surface (as shown in Fig. 5) have been discussed [6]. An embossed honeycomb design showed an improvement in solar absorption by about 3.7–22.9% for radiation at angles varying from  $15^\circ$  to  $70^\circ$ . Toughened aluminum is a good material choice for these absorber surfaces. The absorptivity ( $\alpha$ ) to emissivity ( $\epsilon$ ) ratio is increased by using a thin coating of special black nickel.

Winston et al. [20] described the fabrication, testing and application of the integrated compound parabolic concentrator (ICPC) which integrates a CPC into an evacuated glass tube collector thereby eliminating the need for additional mechanical structure. An array of 336 ICPC collectors ( $100 \text{ m}^2$  area) are used to drive a 20-ton double effect absorption type chiller.

### 3.1.3. Thermal performance of CPCs

A detailed thermal analysis describing the radiative, convective and conductive heat transfer in CPCs along with interplay between them was carried out by Rabl [21]. The convective heat loss is predominant in CPCs with selective absorber coating while radiative heat loss tends to dominate in CPCs with non-selective absorber coating. Using either selective coating or microcavity surface structure for the absorber will increase the absorption, however using both is counter-productive. The paper also warns against heat loss through a potential cooling fin effect created by conductive reflector material (especially when using aluminum sheet).

The thermal performance of the CPC with a flat one-sided absorber has been theoretically analyzed where in the effect of various design parameters (fluid flow rate, inlet temperature, CPC length, selective absorber coating, mirror reflectance etc.) were discussed [22]. The daily efficiency of the collector increased with the fluid flow rate, whereas it decreased with the increase in the inlet temperature and the trough length of the CPC. The selective absorber coating and mirror reflectance are more effective in cases when the solar radiation collection peaks (around solar noon time).

### 3.1.4. Truncation of CPCs

The major disadvantage of a CPC is the larger depth at higher concentrations. For instance, a CPC with concentration ratio of 10 has a reflector-to-aperture area ratio of 11. While this number in case of a simple parabolic concentrator is around 1.1–1.2 [21]. Hence, the CPCs are often truncated (from the aperture end where the slope of parabolas is relatively parallel to the optical axis) to reduce the material costs involved with the reflector surface, and change the depth of the collector. Truncation is done at the expense of decrease in maximum concentration ratio while it increases the acceptance angle. The

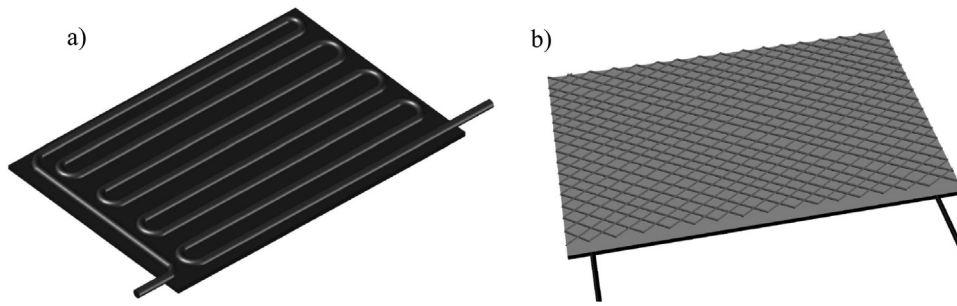


Fig. 5. a) Bottom tube sheet and b) Top embossed surface [6].

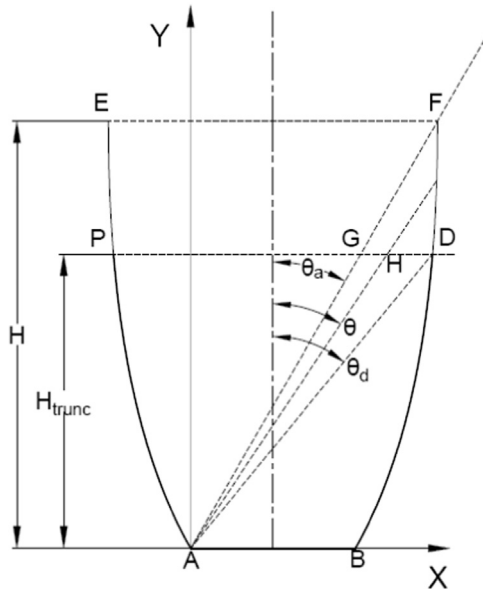


Fig. 6. Truncated CPC with flat absorber [23].

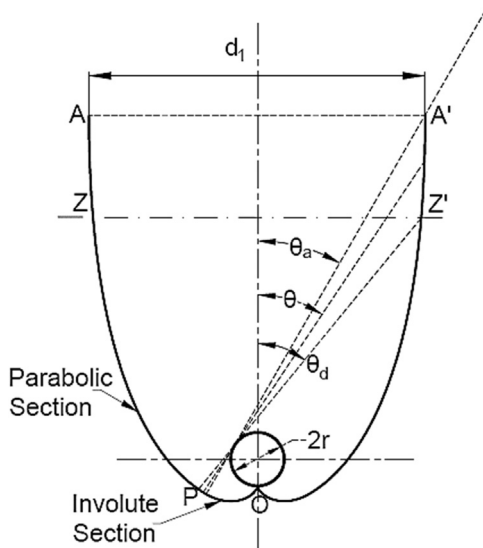


Fig. 7. Truncated CPC with cylindrical absorber [23].

relationship between the amount of truncation, the concentration ratio and the angular acceptance of radiation is established [23]. An angular acceptance function –  $F(\theta)$ , varying between 0 and 1, was used to determine the amount of radiation accepted by a truncated CPC depending on the angle of incidence ( $\theta$ ) of the radiation. For a truncated CPC with flat absorber geometry (refer to Fig. 6), the function  $F(\theta)=1$  and has complete acceptance of radiation below the

original acceptance angle ( $\theta_a$ ) corresponding to the full CPC. In a case when the incident radiation is beyond the original acceptance angle ( $\theta_a$ ) and not exceeding the truncated CPC's edge ray angle ( $\theta_d$ ), all the radiation directly incident on the absorber is accepted while all the radiation intercepted by the reflector is rejected. In this case, the function  $F(\theta)=\frac{1+C}{2C} \left[ 1 - \frac{\tan \theta}{\tan \theta_d} \right]$  where C is the new geometric concentration ratio after truncation. All the radiation beyond the truncated CPC's edge ray angle ( $\theta_d$ ) is rejected and consequently  $F(\theta)=0$ . In case of cylindrical absorber geometry (refer to Fig. 7), there is a change in the angular acceptance function between  $\theta_a$  and  $\theta_d$  which is determined by  $F(\theta)=\frac{1}{2} + \left[ \frac{1 - \left\{ \frac{\sin \theta}{\sin \theta_d} (1 + \pi C \cos \theta_d) \right\}}{2\pi C \cos \theta} \right]$  where C is the new geometric concentration ratio after truncation. The rest of the cases remain same for both flat and cylindrical absorber geometries. A comparison between a truncated CPC with flat absorber and a truncated CPC with cylindrical absorber suggests that the effect of truncation is more prominent in the former with flat absorber.

A detailed analysis on the effects of truncation on geometric parameters, optical and thermal performance of CPCs was presented by Rabl [21]. The equations for calculating the truncated aperture width, height, and the reflector-to-aperture area ratio are mentioned. The method to evaluate average number of reflections inside and outside the original acceptance angle in a truncated CPC is described. The greater the amount of truncation, the lower is the average number of reflections, deviating farther away from the original CPC's average.

### 3.1.5. Fabrication of CPCs

A line-axis CPC with exit aperture width of 0.2 m and acceptance angle of  $36^\circ$  was fabricated using galvanized iron sheets upon which flexible plywood strips glued with mirror material are placed [24]. The whole assembly was encased in an iron channel frame which allowed for inclination adjustments. The absorber used was a black-painted aluminum tube-in-fin type. This CPC accounted for a  $76^\circ\text{C}$  rise in water temperature at no-flow stagnation conditions. Better mirror material and absorber coating would have resulted in further temperature rise.

A two-thirds truncated CPC was fabricated using a dark coated mild steel plate as absorber material and a stainless steel sheet as the reflector material [25]. A low iron glass top cover and acrylic side covers were used to prevent convection losses and soiling of the reflector. A tilt mechanism was incorporated to the frame supporting the whole CPC structure allowing tilt adjustments.

### 3.2. Nonimaging cusp concentrator

Although the cusp concentrator is often referred to as a CPC in the literature, the cusp design comprises two distinct curves that are joined smoothly. The upper part of the cusp geometry is a parabola while the lower part (closer to the cylindrical absorber) is a circular or involute shaped geometry. In either case, the curves are smoothly connected to form the cusp shape. A nonimaging cusp design concentrator was first

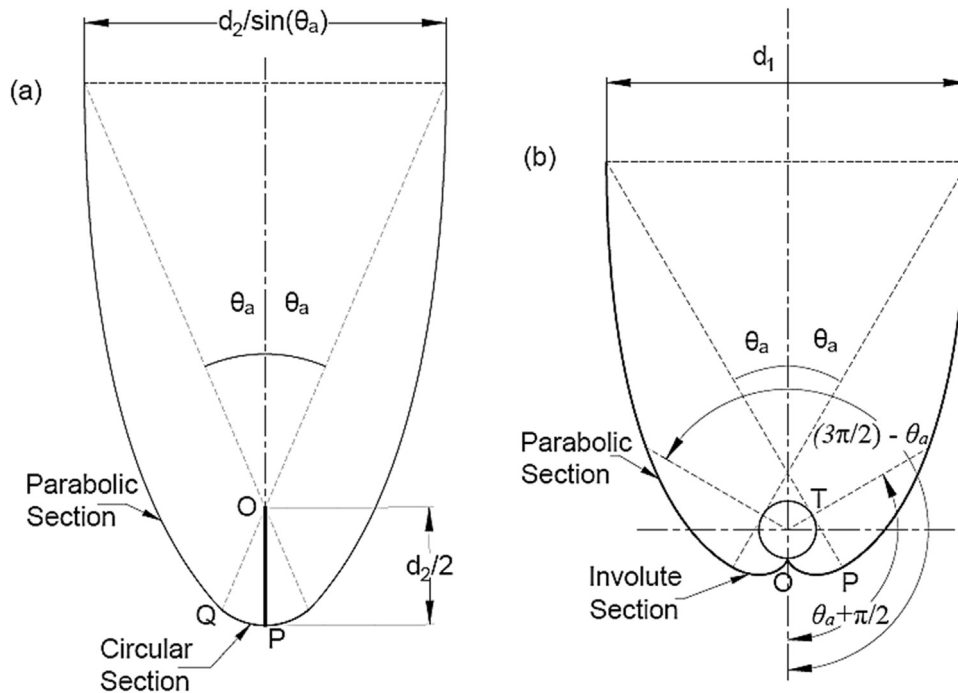


Fig. 8. (a) CPC circular cusp design (b) CPC involute cusp design [27,28].

introduced by Meinel et al. as a patent in 1974 [26]. Winston et al. [27] discussed the circular curvature cusp concentrator (as shown in Fig. 8a) in detail. Rabl [28] analyzed the involute curvature cusp concentrator (as shown in Fig. 8b). He also derived a differential equation to describe an ideal 2D concentrator with arbitrary convex-shaped absorber. As a special case, it was proven that the involute curvature cusp concentrator is the best possible design for cylindrical absorbers.

A CPC cusp design (with a cylindrical absorber) as a stationary concentrator was analyzed experimentally, and it was determined that a 32° acceptance angle stationary CPC could collect solar radiation for 6-h daily at a CR of 1.9 all through the year [29]. Truncation decreases the CR to 1.6 while increasing the acceptance angle to 38.7°.

The thermal performance of the cusp type CPC collector has been analyzed by Hsieh [30]. The effect of various factors (thermal resistance, operating conditions, optical efficiency etc.) on the overall efficiency of the CPC has been discussed. He also recommended that a CPC collector of high concentration ratio should not be installed at geographic locations with high diffuse radiation component owing to the fact that an increased CR lowers the slope as well as the elevation of the CPC efficiency curve. A theoretical numerical model describing the thermal behavior of the CPC cusp type concentrator (with cylindrical absorber) was carried out [31]. The effect of inclination (tilt) when the cusp concentrators are oriented in E-W direction was discussed. The lower the concentration ratio, the more pronounced is the effect of inclination on the CPC collector efficiency. This inverse relationship is attributed to the overwhelming increase in the height and size of the CPC with increasing concentration ratio which in turn suppresses the convective and radiative losses from the absorber and thus, minimizes the effect of inclination. Also, the emphasis of decreasing the convective heat transfer coefficient ( $h_c$ ) in lower inclination CPC collector, which is the dominant contributor to the overall heat transfer coefficient ( $h_{tot}$ ) compared to the radiative ( $h_R$ ) and conductive heat transfer coefficients ( $h_{cd}$ ), was reiterated.

### 3.2.1. Truncation of cusp type concentrators

Similar to the CPCs, the cusp type concentrators also experience ineffective use of the upper portion of the concentrator. Hence for a

practical and cost-effective design, truncation of height is necessary. Truncation of the cusp type nonimaging concentrators (of different acceptance angles) with cylindrical receivers was discussed by McIntire [32]. The plots of height-to-entrance aperture ratio vs. CR and mirror arc length-to-entrance aperture ratio vs. CR are useful guidelines in the design process of mirror substrates of truncated cusp type concentrators.

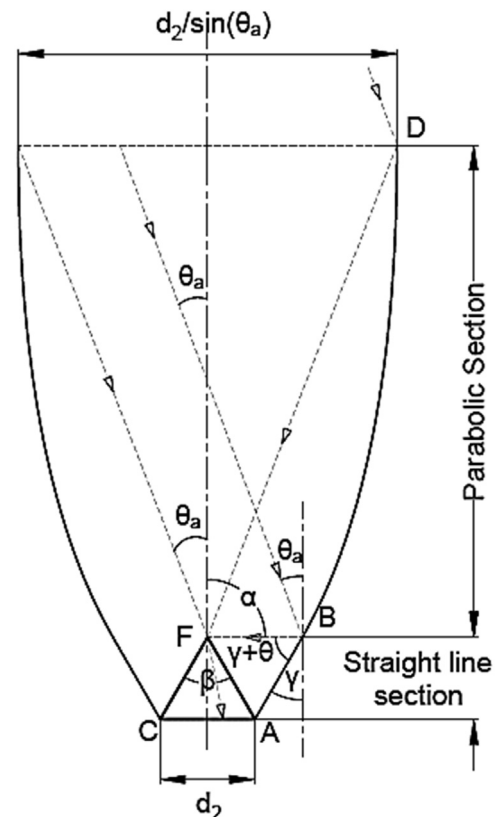


Fig. 9. Prism-coupled compound parabolic concentrator [33].

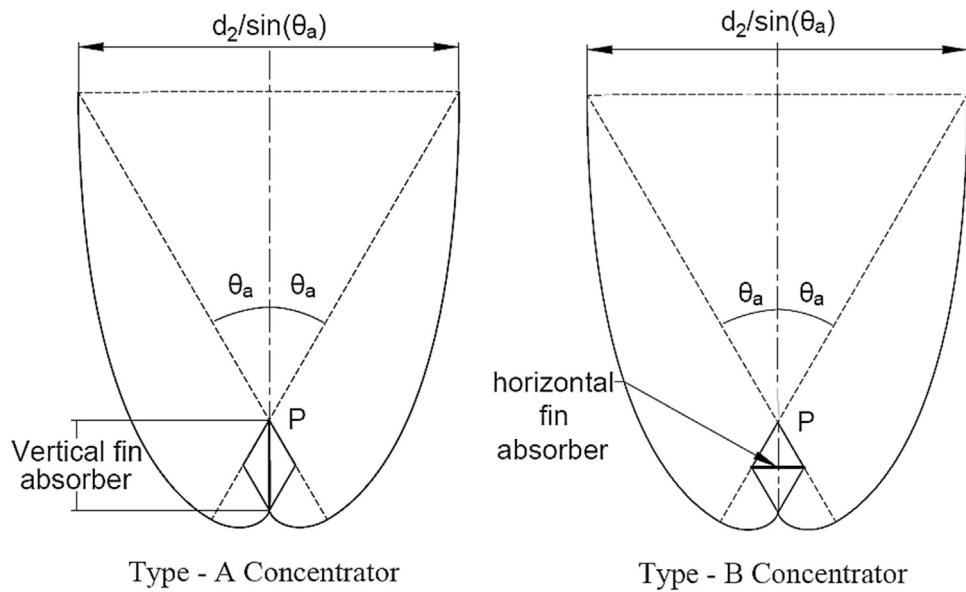


Fig. 10. Type A concentrator with vertical fin absorber and Type B concentrator with horizontal fin absorber [34].

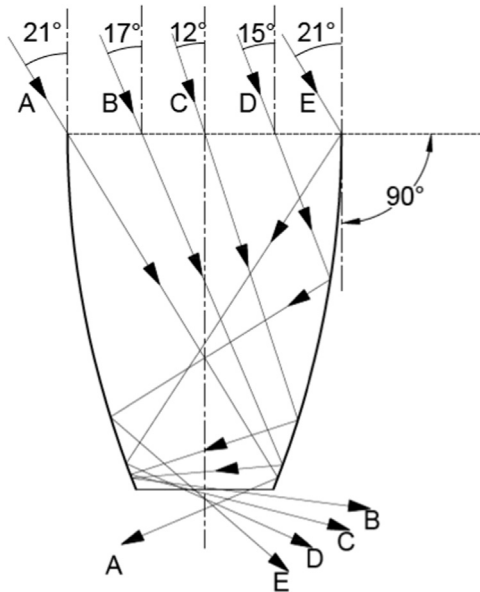


Fig. 11. Near external rays collected by a circular trough of aperture ratio 3.65:1 [36].

3.3. Prism-coupled compound parabolic concentrator

Another nonimaging concentration approach was discussed by Edmonds [33] when he first introduced concept of prism-coupled CPC (PCCPC) to achieve the maximum concentration by a 2D nonimaging concentrator,  $=(\frac{n}{\sin\theta})$ . As shown in Fig. 9, an equilateral prism is positioned at the exit aperture being the base of the prism. There are two sections to the reflector profile - the 'BD' part which a parabola with focus at the apex of the prism - 'F', and the 'AB' part which is a flat line reflector. The angular relationships between the prism apex angle ( $\beta$ ), acceptance angle ( $\theta$ ), refractive index ( $n$ ), angle of the line reflector relative to the axis of symmetry ( $\gamma$ ), and angle at which reflected radiation is incident on the prism surface with respect to the axis of symmetry ( $\alpha$ ) were discussed. The overall conclusion of the theoretical analysis of prism-coupled CPCs show a promising decrement in the length-to-aperture ratio for the same amounts of concentration yielded by regular CPCs or dielectric CPCs with flat absorbers.

Other variations of similar ideas using dielectric material at the absorber level were considered. Two such variations are shown in

Fig. 10A and Fig. 10B where dielectric rhombuses are used encapsulating a fin type absorber in vertical and horizontal position respectively [34]. The nonimaging concentrator used in both these designs is a cusp type concentrator with focus of parabolic profile at the intersection of the edge rays (at vertex 'C') and center of the circular sector profile at vertex 'D'. A theoretical analysis suggested that concentration ratios of 2 ( $\theta_a=41.2^\circ$ , type A) and 1.8 ( $\theta_a=48.8^\circ$ , type B) are possible with higher acceptance angles compared to traditional cusp-fin type collectors. Higher acceptance angles along with slightly lower height-to-aperture ratio make them good candidates for stationary applications.

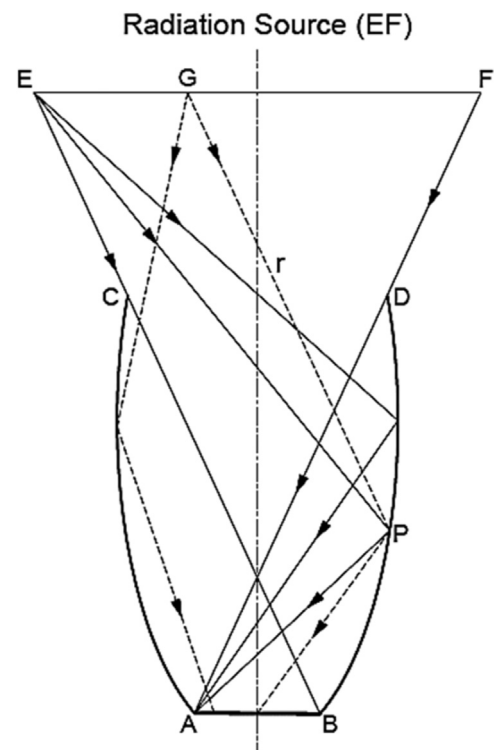


Fig. 12. Compound elliptical concentrator (CEC) [37].

### 3.4. Compound circular arc concentrator (CCAC)

A compound circular arc concentrator (CCAC) is a 2-D non-ideal concentrator wherein the parabolic sections of a comparable CPC are replaced by circular sections [35]. 2-D ideal concentrators (CPCs) obey the relationship  $CR \times \sin(\theta_{max})=1$ , whereas this product is less than unity in the case of 2-D non-ideal concentrators such as CCACs. At low concentration ratios (between 1.5 and 3), the CCACs experienced energy collection somewhat comparable to analogous CPCs and analogous elliptical concentrators (ECs). However, at higher concentrations, the issue of multiple reflections experienced by CCACs limit their optical performance. Nonetheless, CCACs are easier to manufacture using standard sheet metal rollers.

Shapiro also experimented with replacing the parabolic profile of a CPC with a circular arc profile and made an interesting discovery in case of deeper trough CPCs with high concentration ratios [36]. The acceptance half angle of a circular arc profile varied from  $12^\circ$  at the center to  $21^\circ$  at the edge of the input aperture as shown in Fig. 11, whereas, that of a parabolic profile (with same aperture and exit areas of 3.65:1) remained constant at  $16^\circ$  all over the input aperture. Not a significant difference is observed in case of shallow trough CPCs with low concentrations and higher acceptance half angles.

Multiple reflections affecting the performance of the CCACs diurnally as well as through different periods of the year are discussed. A nearly equal performance is reported during hazy weather days and also near dawn and dusk for both profiles. Sometimes, a circular profile is also approximated for a truncated CPC to investigate the comparative performance.

### 3.5. Compound elliptical concentrator (CEC)

The compound elliptical concentrator (CEC) is the design of a nonimaging concentrator where the parabolic profiles in the CPC design are replaced by elliptical profiles. In fact, CPC can be proven as a special case of CEC for an infinite source [37]. The Fig. 12 shows the basic geometry of a CEC in which 'AB' is the absorber while 'EF' is the radiation source. The elliptical profile - 'BD' is part of an ellipse whose foci are 'E' and 'A', and also passing through point 'B'. Similarly the elliptical profile - 'AC' is part of an ellipse whose foci are 'F' and 'B', and also passing through point 'A'.

The application of 3D CEC reflective element (rotational geometry generated by rotation of CEC about the optical axis) as a secondary-stage concentrator in a paraboloidal dish concentrator was investigated using raytracing technique [38]. It is concluded that despite the skew-ray loss due to CEC, it still has better efficiency compared to a trumpet shaped secondary. Furthermore, the compact size of CEC secondary reduces production cost and convective losses while improves its wind resistance.

### 3.6. Dielectric filled nonimaging concentrators

Using a solid or liquid dielectric fill increases the maximum attainable concentration ratio by a factor 'n', where 'n' is the refractive index of the dielectric media that is in the path of radiation between the aperture and the absorber. Dielectric solid fill versions of the nonimaging concentrators need more exploration as they can be potentially strong candidates for stationary applications owing to the fact that they have comparatively higher acceptance angles and, thus, longer diurnal collection of solar energy. However, higher Fresnel reflection losses at the entry aperture for larger incident angles is an issue that needs to be addressed. Applying anti-reflective coatings over the entry aperture can be a partial solution in mitigating this problem. In a simulated analysis, four different dielectric filled nonimaging concentrators namely CPC, CHC, CEC and V-trough were compared with their hollow counterparts as stationary solar concentrators. It is proven that a PMMA dielectric fill would have resulted in a 41–43% increase in diurnal energy

collection during a Summer day in Las Vegas, NV [45].

#### 3.6.1. Dielectric filled lens-V trough (LVT) concentrator

The dielectric filled lens-V trough (LVT) concentrator design as shown in Fig. 13 was experimented with economical dielectric alternatives to plastic and glass – water, mineral oil and a combination of both [39]. A 1.5 mm thick polycarbonate plastic sheet was used to fabricate the outer casing which was then filled with dielectrics. The mineral oil filled LVT (C=2.8) performed better than both the water filled LVT (C=2.4) and combination (water+oil) filled LVT (C=2.8). When oriented in the E-W direction and tested with a PV absorber, the power gain factors of 2.35 and 2.07 were obtained. They performed well even during overcast conditions suggesting a good acceptance of diffuse radiation.

#### 3.6.2. Dielectric compound parabolic concentrator (DCPCs)

A dielectric compound parabolic concentrator (DCPC) is a solid CPC configuration. The CPC profile (2D or 3D) is filled with a dielectric material to create a solid CPC configuration. The concept was introduced mimicking the shape and optical properties of visual receptors in the compound eye of a horseshoe crab [40]. The DCPCs are characterized by their maximum geometric concentration ratio determined by  $1/\left(1 - \frac{2}{n^2}\right)$  for 2D-DCPCs and  $1/\left(1 - \frac{2}{n^2}\right)^2$  for 3D-DCPCs [41]. The full range of angular acceptance  $\theta_{max} \in (0^\circ, 90^\circ)$  can be achieved by  $n$  (refractive index) value ranging from  $\sqrt{2}$  to 2. Such a concentrator would not require any diurnal tracking, just seasonal adjustments. An effective increase in the concentration ratio due to the acceptance of non-normal solar irradiance by an E-W oriented DCPC collector is discussed as an additional benefit of DCPCs which makes them an attractive non-tracking concentrator design [42]. However, the issue of Fresnel reflection associated with refraction at the air-dielectric interface has been neglected. Fresnel reflection lowers the concentration associated with a DCPC design.

DCPCs (acceptance angle= $10.9^\circ$ , acrylic material ( $n=1.5$ )) were tested with PV cell absorbers and a 3.74 times increase in the peak power was observed when compared to a bare cell surface [43]. The end faces of the CPC are slightly inclined at a  $5.5^\circ$  angle to the vertical. This increases the collection of solar radiation when the collector is oriented in E-W direction.

DCPCs are typically used as secondary concentrators due to the dielectric material costs involved. Also, the problem of total internal reflection at the exit aperture-absorber surface interface limited the application of DCPCs. This problem was theoretically addressed by using the principle of frustrated total internal reflection where the

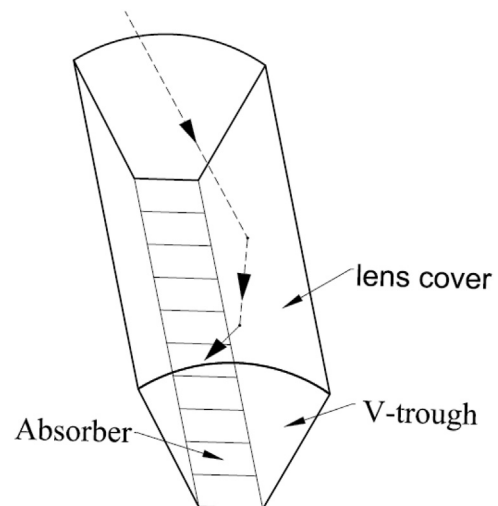


Fig. 13. Dielectric filled lens-V trough concentrator [39].



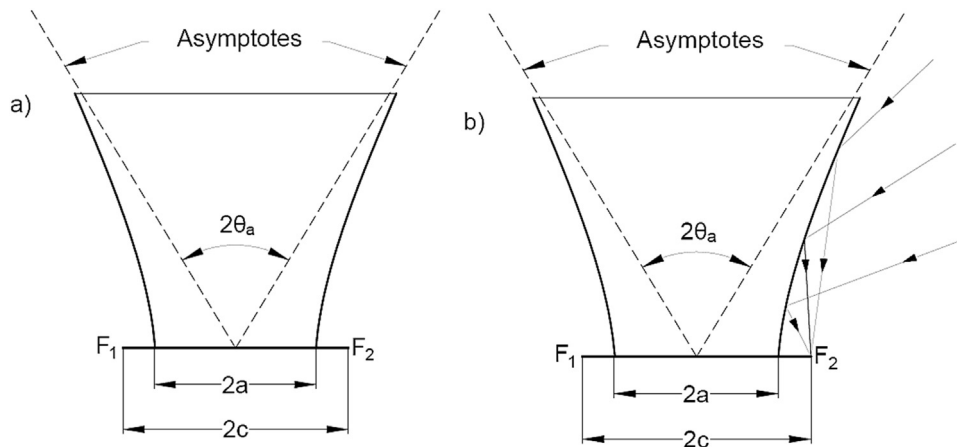


Fig. 14. a) Trumpet shaped concentrator with extreme rays b) showing complementary external extreme rays reach the external absorber (of width  $2c-2a$ ) [50].

absorber is separated by a vacuum gap (less than 200 nm thick) and a slab of same dielectric material [44].

### 3.7. Dielectric total internally reflecting concentrators (DTIRCs)

The DTIRCs were introduced by Ning et al. [46] and they comprised three surfaces – the entry aperture which may be curved, the side walls (with parabolic, hyperbolic or truncated parabolic profiles) which are causing total internal reflection and an exit aperture.

### 3.8. Dielectric asymmetric compound parabolic concentrators (DiACPCs)

Three different truncated designs of dielectric asymmetric compound parabolic concentrators (DiACPCs) with acceptance half angle pairs of ( $0^\circ$  and  $55^\circ$ ), ( $0^\circ$  and  $66^\circ$ ) and ( $0^\circ$  and  $77^\circ$ ) were analyzed using ray-tracing approach for a photovoltaic application at higher northern latitudes ( $> 55^\circ\text{N}$ ) [47]. The distribution of solar irradiance at the absorber surface is non-uniform for direct radiation and, hence, they recommend the usage of DiACPCs to higher latitudes with larger percentage of diffuse radiation. Mallick et al. [48] fabricated an experimental setup by integration of truncated DiACPC ( $0^\circ$  and  $50^\circ$ ) with crystalline-Si photovoltaic cells. The comparative experiments showed a promising improvement in the maximum power output over non-concentrating counterparts by 62% for higher latitude geographical region - Belfast in Northern Ireland ( $54^\circ 36' \text{N}$ ,  $5^\circ 37' \text{W}$ ). Another improvement to a similar design of truncated DiACPC ( $0^\circ$  and  $55^\circ$ ) was proposed [49]. Raytracing and finite element analysis were carried out on the new design where in by adding a reflective film along the bottom edges of the concentrator a 16% increase in the average power output was observed while maintaining cell temperature at  $25^\circ\text{C}$ . However, taking the temperature effects on the PV cell performance into consideration, the increase in the average power output diminished to 6%.

### 3.9. Compound hyperbolic concentrator (CHC)

Compound hyperbolic concentrator (CHC) is the design of a nonimaging concentrator where the parabolic profiles in the CPC design are replaced by two distinct hyperbolic profiles. A trumpet-shaped concentrator is a special type of CHC.

#### 3.9.1. Trumpet-shaped (flowline) concentrator

A trumpet-shaped concentrator has a profile geometry of a single hyperbola as shown in Fig. 14a where  $F_1$  and  $F_2$  are two foci of the hyperbola profile separated by a distance ' $2c$ ' with the exit aperture being ' $2a$ ' and the full-acceptance angle being ' $2\theta_a$ ' (which is also the

asymptote separation angle). The complementary edge-ray string method was used to prove that trumpet-shaped concentrators, CHC and CEC designs are in fact useful ideal concentrators when applied to non-isothermal absorbers and also when preheating by inhomogeneous irradiance of the absorber is preferred [50]. A trumpet shaped concentrator is a reflective surface both on the inside as well as the outside. Notice that the complementary external extreme rays (as shown in Fig. 14b) are aimed at the focus  $F_1$  and reached focus  $F_2$ . All the rays aimed at external absorber at angles greater than  $\theta_a$  will reach the external absorber as shown in Fig. 14b.

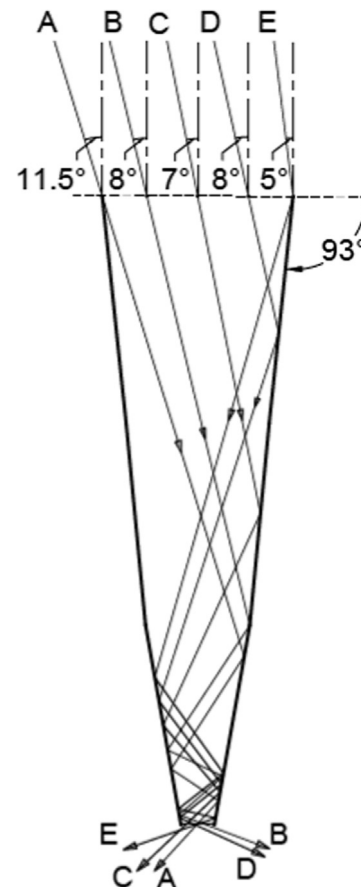


Fig. 15. Polygonal profiled concentrator [36].

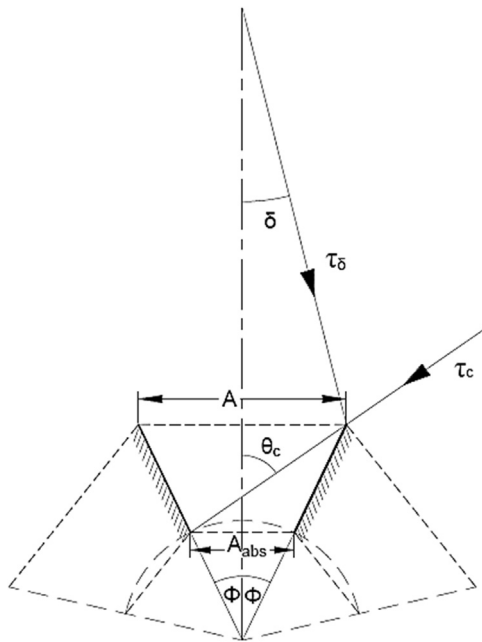


Fig. 16. V-trough concentrator with mirror images and reference circle. The rays  $\tau_\delta$  and  $\tau_c$  have angle of incidence  $\delta$  and  $\theta_c$ , respectively; they pass through the edge of the absorber and are tangential to the reference circle [11].

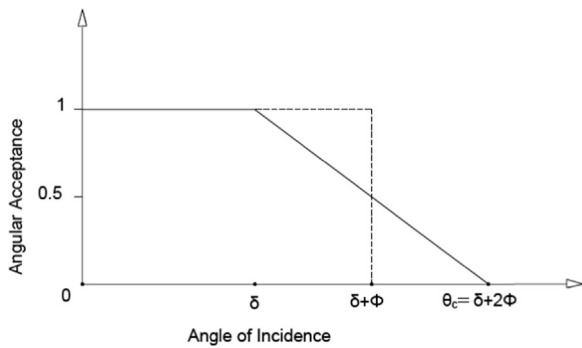


Fig. 17. Angular acceptance of V-trough varying with the angle of incidence [11].

### 3.10. Polygonal and V-trough profile geometry

A polygonal profile (as shown in Fig. 15) instead of a parabolic profile for a CPC was investigated theoretically [36]. An aperture ratio (inlet-to-exit) of 8:1 was used. Two plane mirrors made out of polished metal sheet are bent symmetrically at two equidistant points. The upper segment, the middle segment and the lower segment make  $3^\circ$ ,  $6^\circ$  and  $9^\circ$  bends with respect to the axial plane of the concentrator respectively as shown in the figure below. The acceptance half angle of this concentrator also varied from  $7^\circ$  at the center to  $11^\circ 30'$  at the extremity of the aperture compared to a constant acceptance half angle throughout of  $7^\circ 11'$  for a CPC with parabolic profile. This additional advantage results in the collection of greater amount of radiation at an expense of multiple reflections (up to a maximum of 5 reflections). Hence, the performance of such profile geometry is highly dependent on the reflectance of the mirror material.

The V-trough concentrator geometry is as shown in Fig. 16. The non-hatched surface forms the reflector surface of the V-trough concentrator. Two angles –  $\Phi$  (half angle of the v-shaped cone) and  $\delta$  (complete acceptance angle) – play an important role in determining the amount of energy collected by a V-shaped geometry. One of the following 3 scenarios determines the complete or partial acceptance of the solar radiation by a V-trough concentrator (as shown graphically on Fig. 17).

- i) 100% of all the solar radiation is received within the solid angle  $\delta$  will reach the absorber surface. (provided  $\delta + \Phi < \pi/2$  and  $\Phi < \pi/4$ )
- ii) Beyond the angle  $\delta$ , there is a transition region of width  $2\Phi$  with center at  $\delta + \Phi$ . In this transition region, only part of the received radiation is transmitted to the absorber surface.
- iii) Any radiation beyond the maximum acceptance angle ( $\theta_c = \delta + 2\Phi$ ) is rejected and will never reach the absorber surface.

The geometric concentration ratio for these types of concentrators is given by:

$$CR_{V\text{-trough}} = \frac{1}{\sin(\delta + \Phi)}$$

Similarly,

$$\text{Vertical height of the V-trough, } H_{V\text{-trough}} = \frac{d_1 - d_2}{\sin \Phi}$$

$$\text{Reflector to aperture ratio} = R = \frac{H_{V\text{-trough}}}{d_1} = \frac{1 - \sin(\delta + \Phi)}{\sin \Phi}$$

Previous research has proven that the higher the concentration, the greater is the relative advantage of CPC over the V-trough geometry [11]. At a geometric concentration ratio of 3, the V-trough design seems almost impractical. A quantitative comparison between V-trough and CPC is difficult because of the large number of parameters that should be considered simultaneously. Even disregarding reflector cost and solar energy collection, the comparison involves additional parameters ( $R$  – ratio of reflector to aperture area,  $\langle n \rangle$  – number of reflections, acceptance angle and truncation) besides the value of the concentration ratio. The recent material developments lead to improved reflective surfaces which may improve the overall year round efficiency of a nonimaging CPCs with polygonal or V-type profile compared to parabolic profile in low and medium concentration applications.

### 3.11. Tailored edge-ray concentrators (TERCs)

A further developed extension of the edge-ray principle (also known as simultaneous multiple surface design method) led to the design of the group of concentrators known as the TERCs. They have at least two optically interactive surfaces. These concentrators are named after the optical interactions involved in the transfer of etendue from input aperture to exit aperture ( $R$  stands for refractive, and  $X$  stands for reflective). Viz. an  $RR$  concentrator has both refractive surfaces,  $XR$  concentrator has a reflective surface, and a refractive surface. All the three designs –  $XR$ ,  $RR$  and  $RX$  – are discussed in detail by Miñano et al. [51,52] and are as shown in Fig. 18. The  $XR$  concentrator is an assembly of two pieces – a reflecting element and a refracting element. The  $RR$  concentrator is an aspheric lens. The  $RX$  concentrator is a single piece comprising both refracting and reflecting interfaces. The  $RX$  concentrator requires much more dielectric material than a comparative  $XR$  concentrator and, hence, more suitable in the scenario where the cost of dielectric material is not critical. In general, all these designs perform well under etendue with smaller angular spread i.e. lower acceptance angles. The acceptance angles of these concentrators are generally constrained to less than  $10^\circ$ , this makes them potential candidates for coupling with passive tracking mechanism.

### 3.12. Nonimaging Fresnel lenses

Nonimaging optical sciences were applied to Fresnel lenses and began to be widely used in the field of solar concentration. Fresnel lenses of nonimaging design are usually of convex shape in order to get high concentration ratios and flux distributions with short focal length. The main characteristic of the nonimaging systems is their concentration ratios (i.e. the geometric concentration ratio  $C$ ) which are

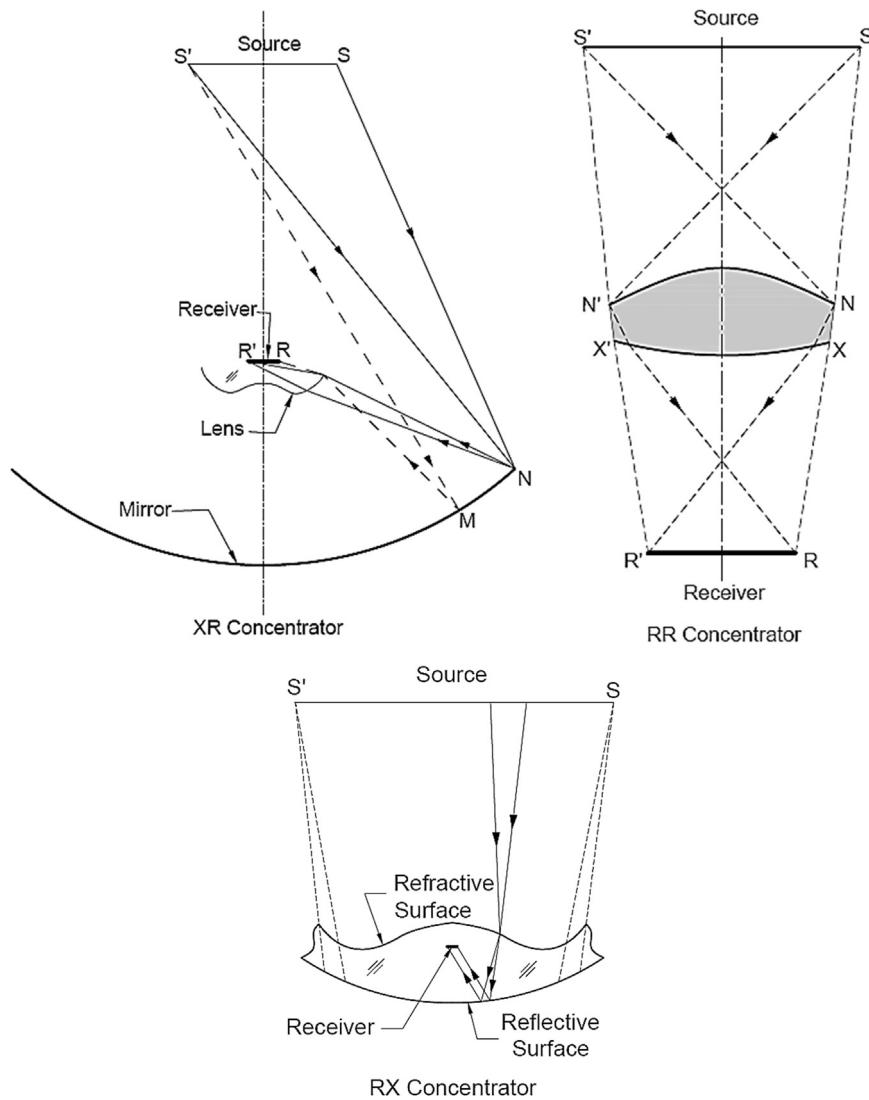


Fig. 18. Tailored edge-ray concentrators (also known as SMS concentrators) – RR, XR and RX designs [8,51,52].

commonly classified as being low for  $C \leq 10$ , or medium for  $10 < C \leq 100$ , or high for  $C > 100$ .

The use of linear convex Fresnel lenses (with acceptance angles  $30^\circ$ ,  $40^\circ$  and  $50^\circ$ ) was investigated using a ray-tracing approach in both E-W and polar orientations [53]. As expected, the focal points were closer together as the acceptance angle decreased which results in a higher temporary concentration. Also, the diurnal movement of the Sun caused focal length shortening. The greater the solar azimuth angle, the shorter is the focal length. Receiver tracking was considered an alternative to overcome this setback. Another alternative approach is to elliptically assemble a series of receivers along the focal path and allow the interaction of working fluid only with those absorbers that are active by using thermostatically controlled valves.

Linear convex Fresnel lens systems were designed to achieve 10X concentration (primary-5X+secondary-2X) with the means of secondary CPC or other non-imaging concentrator [54]. The secondary concentrator also homogenizes the Gaussian distribution of the Fresnel lens concentrated radiation resulting in more homogeneous illumination conditions for PV applications. Light is scattered due to total internal reflection from the facet walls of the individual prismatic elements of a Fresnel lens and is known as the shadowing effect. This causes a loss in the incident radiation which is related to the maximum deflection angle of the lens viz. a maximum deviation of  $10.5^\circ$  reduces the mean annual performance by 7%.

### 3.13. Two-stage or multi-stage nonimaging concentrator

Various nonimaging concentrators such as the CPC, CEC, hyperbolic trumpet shaped concentrator etc. are actively considered as secondary or tertiary optical elements to increase the geometric concentration ratio and/or to fold (decrease) the optical path length [55]. They are particularly useful if higher absorber temperatures are desired and if the primary optical elements (e.g. paraboloidal dish) are susceptible to concentration errors. A nonimaging receiver was proposed for parabolic trough concentrating collectors where an increased overall (thermal+optical) efficiency of 1.4% was observed [56]. Although their absorber design was not cost-effective, it provided improved flux uniformity and increased tolerance towards concentration errors.

Two-stage PV concentrators with a point-focusing Fresnel lens as the primary stage and a dielectric total internally reflecting concentrator (DTIRC) as the secondary stage were discussed by Ning et al. [57]. Both the ray-tracing and the experimental results showed that the two-stage concentrator offered better acceptance angle and higher concentration compared to the point-focusing Fresnel lens alone. Additionally, it also provided a more uniform flux distribution that improved the PV cell performance.

Multistage collection of solar radiation was attempted by Collares-Pereira et al. in 1977 [58]. The collector arrangement is a primary

convex lens and the secondary mirror arrangement. A hyperbolic shaped mirror is used instead of an elliptic shape to achieve better concentration. In order to facilitate fabrication, the shape of the hyperbola can be modified to a V-shaped profile without substantial losses.

#### 4. Recent developments in nonimaging solar optics

Coincidentally, CPC design is a biomimicry of the ommatidium in the compound eye of a horse-shoe crab that evolved millions of years ago. Since the invention and application of the earliest nonimaging concentrator – CPC to collect solar energy, various nonimaging collectors have seen diverse applications as solar energy collectors. Solar-pumped lasers are setup using nonimaging Fresnel lenses [59]. Other applications involve concentrated photovoltaics, solar thermo-photovoltaic systems etc.

##### 4.1. Fields of application

Demonstration of building integrated photovoltaics with a stationary arrangement of nonimaging concentrators was conducted using two different concentrator designs – a linear convex Fresnel lens (10X concentration) and a combination of linear convex Fresnel lens (5X concentration) with CPC (2X concentration) [54].

Buildings in non-seismic, snow accumulation regions (typically higher latitude regions) are most suitable for installing a mid-temperature range (80–250 °C) stationary nonimaging solar collector [60]. Four different nonimaging collector configurations – CPC, sea shell with upper reflector, sea shell with adjustable reflector and vertical asymmetric CPC – coupled with evacuated tubes were considered as a part of a case study for building integration. The suitable building types, structural and reflector details were discussed.

Solar photocatalytic detoxification of water is the removal of hazardous and non-biodegradable wastes using the near-ultraviolet band of the solar spectrum (wavelength under 390 nm). The UV radiation photoexcites a semiconductor catalyst (typically  $\text{TiO}_2$ ) to promote oxidative and reductive reactions. Under the SOLARDETOX project, a detoxification plant was built that incorporated two rows of 21 modules of cusp type CPC collectors (oriented in E-W direction) with a total aperture area of 100  $\text{m}^2$  and a loop capacity of 800 l/cycle [61].

Prospective application of the nonimaging optics in laser fiber optic surgical procedures was discussed [62]. The increase in irradiance with maximum collection efficiency and uniform distribution over a wider angular range are the motivating factors when compared to imaging optics or tapered V-cone type devices.

A lithium bromide-water ( $\text{LiBr-H}_2\text{O}$ ) based solar absorption cooling system was coupled with CPC solar collectors with evacuated tube receivers and tested in Jinan City, China (36.65°N, 117.12°E) [63]. The CPC solar collectors (105  $\text{m}^2$ ) that were oriented in N-S direction at a tilt angle of 20° achieved an average cooling capacity of 9.2 kW at a

COP of 0.19. These systems provided chilled water at 15 °C from 11 A.M. to 3:30 P.M. The thermal efficiency of the CPC collectors were comparatively higher than traditional collector at higher operating fluid (water) temperatures.

##### 4.2. Optical modeling using computer programs

The field of optical modeling has seen tremendous progress in the past two decades due to the exponential increase in computing power. Early optical modeling efforts on CPCs involved using multiple programs to achieve the desired ray-tracing results. Viz. AutoCAD was used in conjunction with LOTUS 1–2–3 and FORTRAN to model and ray-trace a cusp-type CPC with cylindrical absorber [64].

Currently, there are commercially available optical modeling software that can be handy in optical modeling of various designs. These programs can be broadly classified into 3 categories: sequential ray-tracing type, non-sequential ray-tracing type and finite-difference time-domain (FDTD) simulation type. Sequential ray-tracing software interacts with the light from a user-defined source in a sequentially defined manner. Each surface in the optical system interacts with the light one at a time in the order defined by the user. These type of programs are typically used to model optical systems such as cameras, endoscopes, microscopes, telescopes etc. Examples of such programs are CODE V, ASAP etc. On the other hand, non-sequential programs allow the ray interaction with any surface multiple times without any predetermined sequence. Ray-scattering and Fresnel reflections are effectively accounted for, leading to more accurate modeling of real world interactions. Some non-sequential optical modeling programs can also model coherent systems through the Gaussian beam summation method. These type of programs are typically used to model imaging systems, light pipes, backlights, luminaires etc. Examples of such programs are Optics Lab, ZEMAX, OSLO, TracePro, FRED, Light Tools etc. When the size of the optical system shrinks to the wavelength-scale, the Gaussian beam summation modeling breaks down. That is when FDTD programs come in handy. They solve for Maxwell's equations to propagate electro-magnetic fields through micro and nano-scale optical systems. Examples of such programs are Virtual Lab, SPEOS etc [65].

Optical simulation software such as TracePro, OptiCAD and ASAP had been reportedly used to simulate the performance of nonimaging Fresnel lens or nonimaging optics in general [44,66]. Optimization algorithms are frequently embedded in these types of software to perform design optimization of a newer design. OptiCAD was used to compare the optical performance of a linear Fresnel lens (10X concentration), and a hybrid system of linear Fresnel (5X concentration)+CPC (2X concentration) [37]. This 3D analysis showed the effect of transverse and longitudinal angles on focus and the optical concentration ratio. The hybrid system of 5X linear Fresnel lens +2X CPC proved more effective for stationary applications (BIPV in this case).

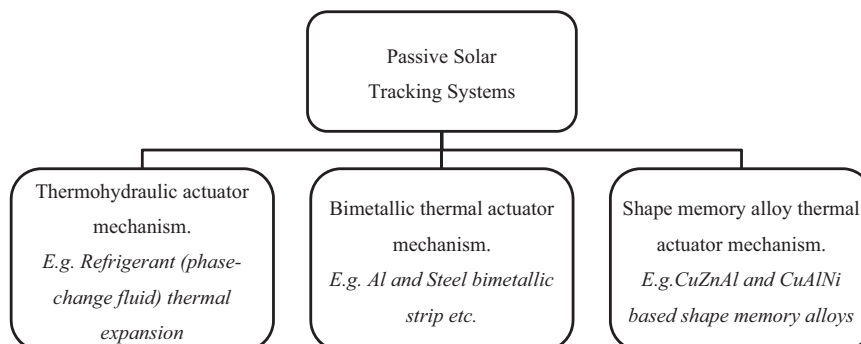


Fig. 19. Classification of passive tracking systems.

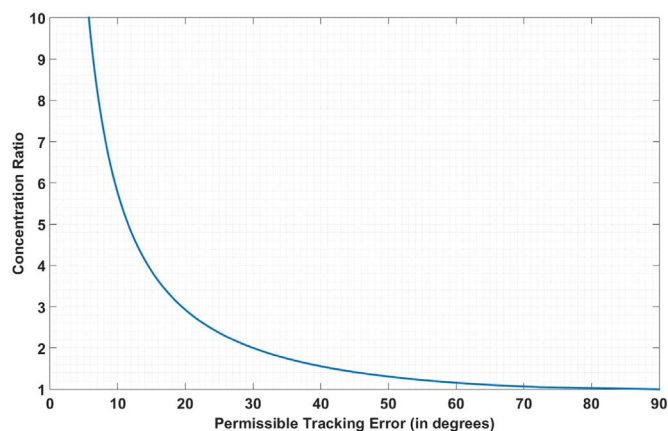


Fig. 20. Permissible single-axis tracking error vs. the concentration ratio for a hollow CPC design.

## 5. Passive-tracking nonimaging systems

As the focus of this paper is on stationary and passive nonimaging concentration systems, it is only relevant to include some discussion on advancements in passive solar tracking systems. They are a particularly attractive option owing to their simplistic, low-cost design. As opposed to the active solar tracking mechanism which uses certain portion of the auxiliary power (electrical power) to drive its tracking mechanism, the passive tracking mechanism is driven by changing physical attributes due to the diurnal motion of the sun.

Passive tracking systems are based on differential thermal expansion of materials such as refrigerants, bimetallic strips or shape memory alloys. The mechanism usually comprises two actuators working against each other. When there is unequal illumination of the actuators, there are unbalanced forces causing the orientation of the apparatus in such a direction where equal illumination of actuators and the balance of the forces are restored. They are inexpensive and less complex compared to active trackers but are also less efficient. Also, since they are thermally activated mechanisms, ambient temperature variations can affect their functionality. Clifford et al. [67] designed a passive solar tracking system which increased the energy output of the solar panels by 23% compared to a fixed system. However, incorporating a night return mechanism and a dual axis tracking mechanism are the future challenges for this design. The drying time of coffee beans is reduced by 2–3 days using a manually adjustable (with 15° increment) single-axis tracking system [68]. Shape memory alloy actuators were used to design a passive tracking system. A tracking accuracy of  $\pm 5^\circ$  was achieved using these systems. The inherent disadvantage of less precise tracking of passive tracking systems can be overcome by coupling with nonimaging optics. The most popular passive tracking mechanisms are classified as shown in Fig. 19 [67–70].

The acceptance angle of a nonimaging concentrator can be the maximum permissible tracking error for a passive tracking system oriented in N-S direction. Fig. 20 shows the practical concentration ratio attainable as a function of the maximum permissible tracking error in case of a CPC. Hence, given the low-cost of the passive tracking systems, coupling them with nonimaging concentrators is a viable option to achieve low to moderate concentrations.

## 6. Conclusions

An exhaustive review given here of the nonimaging concentrators introduces the reader to various types of concentrator geometries. The discussed designs include the CPC, truncated CPC, cusp concentrator, prism-coupled CPC, CCAC, CEC, DCPC, DTIRC, DiACPC, CHC, trumpet-shaped concentrator, polygonal profile concentrator, V-trough

profile concentrator, TERCs, nonimaging Fresnel lens, two-stage and multi-stage nonimaging concentrators. Most of these concentrator designs perform well as stationary or passive tracking concentrators for low to medium concentration ratios (1–3X and 3–10X). Multi-stage concentrators show the versatile usefulness of nonimaging concentrators not only in achieving higher concentration but also in achieving it economically. However, care must be taken not to go lower than  $3^\circ$  acceptance angle while designing a passive tracking nonimaging concentrator as it affects circumsolar radiation collection, an important design criteria to consider when coupling with passive tracking systems. Dielectric solid fill versions of the nonimaging concentrators are potentially strong candidates for stationary applications as they have comparatively higher acceptance angles and, thus, longer diurnal collection of solar energy. However, higher Fresnel reflection losses at the entry aperture for larger incident angles is an issue that needs to be addressed more effectively as anti-reflective coatings can only be partial solutions. This paper also discusses various novel applications of nonimaging collectors from integration in BiPVs to the solar photocatalytic detoxification of water. Finally, some of the recent developments in ray-tracing algorithms that help in optical modeling of nonimaging concentrators, and passive tracking technologies that can be potentially coupled with nonimaging concentrators are also discussed.

## References

- [1] Janet L. Sawin, Kristin Seyboth, Freyr Sverrisson FA, Adam Brown, Bärbel Epp, Anna Leidreiter, Christine Lins, Hannah E. Murdock, et al. Renewables 2016 global status report. Paris; 2016. [doi: ISBN 978-3-9818107-0-7].
- [2] NREL-SolarPACES. NREL: Concentrating solar power projects – concentrating solar power projects by project name. Webpage 2016. ([http://www.nrel.gov/csp/solarpaces/by\\_project.cfm](http://www.nrel.gov/csp/solarpaces/by_project.cfm)) [accessed 24.10.16].
- [3] Pitz-Paal R. Chapter 19 – solar energy – concentrating solar power. Future Energy 2014;405–31. <http://dx.doi.org/10.1016/B978-0-08-099424-6.00019-3>.
- [4] Gleckman P, O’Gallagher J, Winston R. Concentration of sunlight to solar-surface levels using non-imaging optics. Nature 1989;339:198–200. <http://dx.doi.org/10.1038/339198a0>.
- [5] Jones GG, Bouamane L. Power from sunshine: a business history of solar energy. Harvard Bus Sch Work Pap;No. 12–105; 2012.
- [6] Kapany NS. Current status and future prospects of non-tracking solar collectors. Proc SPIE 1976;68:77–84. <http://dx.doi.org/10.1117/12.978105>.
- [7] Chong KK, Chay KG, Chin KH. Study of a solar water heater using stationary V-trough collector. Renew Energy 2012;39:207–15. <http://dx.doi.org/10.1016/j.renene.2011.08.002>.
- [8] Winston R, Miñano JC, Benítez P, Shatz N, Bortz JC. Nonimaging Optics. Burlington, Massachusetts: Elsevier Academic Press; 2005. <http://dx.doi.org/10.1016/B978-012759751-5/50004-X>.
- [9] Ries H, Rabl A. Edge-ray principle of nonimaging optics. J Opt Soc Am A 1994;11:2627–32. <http://dx.doi.org/10.1364/JOSAA.11.002627>.
- [10] Gordon JM, Rabl A. Nonimaging compound parabolic concentrator-type reflectors with variable extreme direction. Appl Opt 1992;31:7332–8. <http://dx.doi.org/10.1364/AO.31.007332>.
- [11] Rabl A. Comparison of solar concentrators. Sol Energy 1976;18:93–111. [http://dx.doi.org/10.1016/0038-092X\(76\)90043-8](http://dx.doi.org/10.1016/0038-092X(76)90043-8).
- [12] O’Gallagher JJ. Retrospective on 30 years of nonimaging optics development for solar energy at the University of Chicago. Proc SPIE 2016;9955:995504–20. <http://dx.doi.org/10.1117/12.2238637>.
- [13] Khamooshi M, Salati H, Egelioglu F, Hooshyar Faghiri A, Tarabishi J, Babadi S. A review of solar photovoltaic concentrators. Int J Photo 2014;2014:17. <http://dx.doi.org/10.1155/2014/958521>.
- [14] Chong K-K, Lau S-L, Yew T-K, Tan PC-L. Design and development in optics of concentrator photovoltaic system. Renew Sustain Energy Rev 2013;19:598–612. <http://dx.doi.org/10.1016/j.rser.2012.11.005>.
- [15] Winston R. Principles of solar concentrators of a novel design. Sol Energy 1974;16:89–95. [http://dx.doi.org/10.1016/0038-092X\(74\)90004-8](http://dx.doi.org/10.1016/0038-092X(74)90004-8).
- [16] Grimmer DP. A comparison of compound parabolic and simple parabolic concentrating solar collectors. Sol Energy 1979;22:21–5. [http://dx.doi.org/10.1016/0038-092X\(79\)90055-0](http://dx.doi.org/10.1016/0038-092X(79)90055-0).
- [17] Rönnelid M, Perers B, Karlsson B. Construction and testing of a large-area CPC-collector and comparison with a flat plate collector. Sol Energy 1996;57:177–84. [http://dx.doi.org/10.1016/S0038-092X\(96\)00062-X](http://dx.doi.org/10.1016/S0038-092X(96)00062-X).
- [18] O’Gallagher JJ. Nonimaging optics in solar energy. Synth Lect Energy Environ Technol Sci Soc 2008;2:1–120. <http://dx.doi.org/10.2200/S00120ED1V01Y200807EGY002>.
- [19] Azhari AA, Khonkar HE. A thermal comparison performance of CPC with modified (dual-cavity) and non-modified absorber. Renew Energy 1996;9:584–8. [http://dx.doi.org/10.1016/0960-1481\(96\)88357-1](http://dx.doi.org/10.1016/0960-1481(96)88357-1).
- [20] Winston R, O’Gallagher JJ, Duff WS, Cavallaro A. The integrated compound

- parabolic concentrator: from development to demonstration. Boulder, CO (United States): American Solar Energy Society; 1997.
- [21] Rabl A. Optical and thermal properties of compound parabolic concentrators. *Sol Energy* 1976;18:497–511. [http://dx.doi.org/10.1016/0038-092X\(76\)90069-4](http://dx.doi.org/10.1016/0038-092X(76)90069-4).
- [22] Tchinda R, Ngos N. A theoretical evaluation of the thermal performance of CPC with flat one-sided absorber. *Int Commun Heat Mass Transf* 2006;33:709–18. <http://dx.doi.org/10.1016/j.icheatmasstransfer.2006.01.019>.
- [23] Carvalho MJ, Collares-Pereira M, Gordon JM, Rabl A. Truncation of CPC solar collectors and its effect on energy collection. *Sol Energy* 1985;35:393–9. [http://dx.doi.org/10.1016/0038-092X\(85\)90127-6](http://dx.doi.org/10.1016/0038-092X(85)90127-6).
- [24] Yadav YP, Yadav AK, Anwar N, Eames PC, Norton B. The fabrication and testing of a line-axis compound parabolic concentrating solar energy collector. *Renew Energy* 1996;9:572–5. [http://dx.doi.org/10.1016/0960-1481\(96\)88354-6](http://dx.doi.org/10.1016/0960-1481(96)88354-6).
- [25] Sheth MG, Shah PK. Design and development of compound parabolic concentrating solar collector with flat plate absorber. *Int J Innov Res Sci Eng Technol* 2013;2:3384–9.
- [26] Meinel AB, Meinel MP, Trombe F. *Applied solar energy: an introduction*. Mass: Addison-Wesley, Reading; 1976. p. 207. [n.d.].
- [27] Winston R, Hinterberger H. Principles of cylindrical concentrators for solar energy. *Sol Energy* 1975;17:255–8. [http://dx.doi.org/10.1016/0038-092X\(75\)90007-9](http://dx.doi.org/10.1016/0038-092X(75)90007-9).
- [28] Rabl A. Solar concentrators with maximal concentration for cylindrical absorbers. *Appl Opt* 1976;15:1871–3. <http://dx.doi.org/10.1364/AO.15.001871>.
- [29] Manrique JA. A compound parabolic concentrator. *Int Commun Heat Mass Transf* 1984;11:267–73. [http://dx.doi.org/10.1016/0735-1933\(84\)90042-3](http://dx.doi.org/10.1016/0735-1933(84)90042-3).
- [30] Hsieh CK. Thermal analysis of CPC collectors. *Sol Energy* 1981;27:19–29. [http://dx.doi.org/10.1016/0038-092X\(81\)90016-5](http://dx.doi.org/10.1016/0038-092X(81)90016-5).
- [31] Norton B, Kothdiwala AF, Eames PC. Effect of inclination on the performance of CPC solar energy collectors. *Renew Energy* 1994;5:357–67. [http://dx.doi.org/10.1016/0960-1481\(94\)90397-2](http://dx.doi.org/10.1016/0960-1481(94)90397-2).
- [32] McIntire WR. Truncation of nonimaging cusp concentrators. *Sol Energy* 1979;23:351–5. [http://dx.doi.org/10.1016/0038-092X\(79\)90130-0](http://dx.doi.org/10.1016/0038-092X(79)90130-0).
- [33] Edmonds IR. Prism-coupled compound parabola: a new ideal and optimal solar concentrator. *Opt Lett* 1986;11:490–2. <http://dx.doi.org/10.1364/OL.11.000490>.
- [34] Bloisi F, Cavaliere P, De Nicola S, Martellucci S, Vicari L, Quartieri J. Ideal nonfocusing concentrator with fin absorbers in dielectric rhombuses. *Opt Lett* 1987;12:453–5.
- [35] Jones RE, Anderson GC. Optical properties of compound circular arc concentrators. *Sol Energy* 1978;21:149–51. [http://dx.doi.org/10.1016/0038-092X\(78\)90042-7](http://dx.doi.org/10.1016/0038-092X(78)90042-7).
- [36] Shapiro MM. Non-focussing solar concentrators of easy manufacture. *Sol Energy* 1977;19:211–3. [http://dx.doi.org/10.1016/0038-092X\(77\)90061-5](http://dx.doi.org/10.1016/0038-092X(77)90061-5).
- [37] Chaves J. *Introduction to Nonimaging Optics*, Second edition. Boca Raton, Florida: CRC Press; 2015. <http://dx.doi.org/10.1201/b18785>.
- [38] Kritchman EM. Second-stage CEC concentrator. *Appl Opt* 1982;21:751–4. <http://dx.doi.org/10.1364/AO.21.000751>.
- [39] Edmonds IR, Cowling IR, Chan HM. The design and performance of liquid filled stationary concentrators for use with photovoltaic cells. *Sol Energy* 1987;39:113–22. [http://dx.doi.org/10.1016/S0038-092X\(87\)80039-7](http://dx.doi.org/10.1016/S0038-092X(87)80039-7).
- [40] Levi-Setti R, Park DA, Winston R. The conical cones of Limulus as optimised light concentrators. *Nature* 1975;253:115–6.
- [41] Winston R. Dielectric compound parabolic concentrators. *Appl Opt* 1976;15:291–2. <http://dx.doi.org/10.1364/AO.15.000291>.
- [42] Scharlack RS. All-dielectric compound parabolic concentrator. *Appl Opt* 1977;16:2601–2. <http://dx.doi.org/10.1364/AO.16.002601>.
- [43] Goodman NB, Ignatius R, Wharton L, Winston R. Solid-dielectric compound parabolic concentrators: on their use with photovoltaic devices. *Appl Opt* 1976;15:2434–6. <http://dx.doi.org/10.1364/AO.15.002434>.
- [44] Hull JR. Dielectric compound parabolic concentrating solar collector with a frustrated total internal reflection absorber. *Appl Opt* 1989;28:157–62. <http://dx.doi.org/10.1364/AO.28.000157>.
- [45] Madala S, Boehm RF. Effect of reflection losses on stationary dielectric-filled nonimaging concentrators. *J Photonics Energy* 2016;6:47002. <http://dx.doi.org/10.1117/1.JPE.6.047002>.
- [46] Ning X, Winston R, O'Gallagher J. Dielectric totally internally reflecting concentrators. *Appl Opt* 1987;26:300–5. <http://dx.doi.org/10.1364/AO.26.000300>.
- [47] Sarmah N, Richards BS, Mallick TK. Evaluation and optimization of the optical performance of low-concentrating dielectric compound parabolic concentrator using ray-tracing methods. *Appl Opt* 2011;50:3303–10. <http://dx.doi.org/10.1364/AO.50.003303>.
- [48] Mallick TK, Eames PC, Norton B. Non-concentrating and asymmetric compound parabolic concentrating building façade integrated photovoltaics: an experimental comparison. *Sol Energy* 2006;80:834–49. <http://dx.doi.org/10.1016/j.solener.2005.05.011>.
- [49] Baig H, Sarmah N, Chemisana D, Rosell J, Mallick TK. Enhancing performance of a linear dielectric based concentrating photovoltaic system using a reflective film along the edge. *Energy* 2014;73:177–91. <http://dx.doi.org/10.1016/j.energy.2014.06.008>.
- [50] Gordon JM. Complementary construction of ideal nonimaging concentrators and its applications. *Appl Opt* 1996;35:5677–82. <http://dx.doi.org/10.1364/AO.35.005677>.
- [51] Miñano JC, González JC. New method of design of nonimaging concentrators. *Appl Opt* 1992;31:3051–60. <http://dx.doi.org/10.1364/AO.31.003051>.
- [52] Miñano JC, Benítez P, González JC. RX: a nonimaging concentrator. *Appl Opt* 1995;34:2226–35. <http://dx.doi.org/10.1364/AO.34.002226>.
- [53] Kritchman EM, Friesem AA, Yekutieli G. A fixed Fresnel lens with tracking collector. *Sol Energy* 1981;27:13–7. [http://dx.doi.org/10.1016/0038-092X\(81\)90015-3](http://dx.doi.org/10.1016/0038-092X(81)90015-3).
- [54] Chemisana D, Ibáñez M, Barrau J. Comparison of Fresnel concentrators for building integrated photovoltaics. *Energy Convers Manag* 2009;50:1079–84. <http://dx.doi.org/10.1016/j.enconman.2008.12.002>.
- [55] Jaffe LD, Poon PT. Secondary and compound concentrators for parabolic dish solar thermal power systems; 1981.
- [56] Gee R, Cohen G, Winston R. A nonimaging receiver for parabolic trough concentrating collectors. *ASME Sol. In: Proceedings of the 2002 international solar energy conference*; 2002. p. 269–76.
- [57] Ning X, O'Gallagher J, Winston R. Optics of two-stage photovoltaic concentrators with dielectric second stages. *Appl Opt* 1987;26:1207–12. <http://dx.doi.org/10.1364/AO.26.001207>.
- [58] Collares-Pereira M, Rabl A, Winston R. Lens-mirror combinations with maximal concentration. *Appl Opt* 1977;16:2677–83. <http://dx.doi.org/10.1364/AO.16.002677>.
- [59] Xie WT, Dai YJ, Wang RZ, Sumathy K. Concentrated solar energy applications using Fresnel lenses: a review. *Renew Sustain Energy Rev* 2011;15:2588–606. <http://dx.doi.org/10.1016/j.rser.2011.03.031>.
- [60] Goodman JH. Building interior evacuated tubes and reflectors. In: *Proceedings of the Sol. 2009 ASES conference*. Buffalo, NY; 2009.
- [61] Blanco J, Malato S, Fernández P, Vidal A, Morales A, Trincado P, et al. Compound parabolic concentrator technology development to commercial solar detoxification applications. *Sol Energy* 1999;67:317–30. [http://dx.doi.org/10.1016/S0038-092X\(00\)00078-5](http://dx.doi.org/10.1016/S0038-092X(00)00078-5).
- [62] Gordon JM. Nonimaging optical designs for laser fiber optic surgery. *Opt Eng* 1998;37:539–42. <http://dx.doi.org/10.1117/1.601642>.
- [63] Lu ZS, Wang RZ, Xia ZZ, Lu XR, Yang CB, Ma YC, et al. Study of a novel solar adsorption cooling system and a solar absorption cooling system with new CPC collectors. *Renew Energy* 2013;50:299–306. <http://dx.doi.org/10.1016/j.renene.2012.07.001>.
- [64] Khonkar HEI, Sayigh AAM. Raytrace for compound parabolic concentrator. *Renew Energy* 1994;5:376–83. [http://dx.doi.org/10.1016/0960-1481\(94\)90400-6](http://dx.doi.org/10.1016/0960-1481(94)90400-6).
- [65] Optical Software: Which Program is Right for Me? 2006. (<http://optics.org/article/25404>) [accessed 01.01.15].
- [66] Lin J-S, Huang W-C, Hsu H-C, Chang M-W, Liu C-P. A study for the special Fresnel lens for high efficiency solar concentrators. *Nonimaging Opt Effic Illum Syst II* 2005;5942:59420X1. <http://dx.doi.org/10.1117/12.614298>.
- [67] Clifford MJ, Eastwood D. Design of a novel passive solar tracker. *Sol Energy* 2004;77:269–80. <http://dx.doi.org/10.1016/j.solener.2004.06.009>.
- [68] Poulek V. Testing the new solar tracker with shape memory alloy actuators. In: *Photovolt Energy Conversion, 1994, Conf Rec Twenty Fourth, IEEE Photovolt Spec Conf - 1994, 1994 IEEE First World Conf vol. 1*; 1994. p. 1131–3. doi: (<http://doi.org/10.1109/WCPEC.1994.520161>).
- [69] Klotz FH, Mohring HD, Gruel C, Abella MA, Sherborne J, Bruton T, et al. Field test results of the Archimedes Photovoltaic V-Trough concentrator system. In: *Proc. 17th Eur Photovolt Sol Energy Conf Exhib Munich, Ger*; 2001. p. 492–5.
- [70] Sánchez MMP, Tamayo DB, Estrada RHC. Design and construction of a dual axis passive solar tracker, for use on Yucatán. In: *ASME 2011 5th Int Conf Energy Sustain*; 2011. p. 1341–6.